

FACT - Threshold prediction for higher duty cycle and improved scheduling

T. BRETZ¹, A. BILAND¹, J. BUSS², D. DORNER³, S. EINECKE², D. EISENACHER³, D. HILDEBRAND¹, M. L. KNOETIG¹, T. KRÄHENBÜHL¹, W. LUSTERMANN¹, K. MANNHEIM³, K. MEIER³, D. NEISE², A.-K. OVERKEMPING², A. PARAVAC³, F. PAUSS¹, W. RHODE², M. RIBORDY⁴, T. STEINBRING³, F. TEMME², J. THAELE², P. VOGLER¹, R. WALTER⁵, Q. WEITZEL¹, M. ZÄNGLEIN³ (FACT COLLABORATION)

¹ETH Zurich, Switzerland – Institute for Particle Physics, Schafmattstr. 20, 8093 Zurich

²Technische Universität Dortmund, Germany – Experimental Physics 5, Otto-Hahn-Str. 4, 44221 Dortmund

³Universität Würzburg, Germany – Institute for Theoretical Physics and Astrophysics, Emil-Fischer-Str. 31, 97074 Würzburg,

⁴EPF Lausanne, Switzerland – Laboratory for High Energy Physics, 1015 Lausanne

⁵University of Geneva, Switzerland – ISDC Data Center for Astrophysics, Chemin d'Ecogia 16, 1290 Versoix

thomas.bretz@phys.ethz.ch

Abstract: The First G-APD Cherenkov telescope (FACT) is the first telescope using silicon photon detectors (G-APD aka. SiPM). The use of Silicon devices promise a higher photon detection efficiency, more robustness and higher precision than photo-multiplier tubes. Being operated during different light-conditions, the threshold settings of a Cherenkov telescope have to be adapted to feature the lowest possible threshold but also an efficient suppression of triggers from night-sky background photons. Usually this threshold is set either by experience or a mini-ratescan. Since the measured current through the sensors is directly correlated with the noise level, the current can be used to set the best threshold at any time. Due to the correlation between the physical threshold and the final energy threshold, the current can also be used as a measure for the energy threshold of any observation. This presentation introduces a method which uses the properties of the moon and the source position to predict the currents and the corresponding energy threshold for every upcoming observation allowing to adapt the observation schedule accordingly.

Keywords: FACT, G-APD, silicon photo sensor, focal plane

1 Introduction

Since Oct. 2011, the FACT Collaboration is operating the First G-APD Cherenkov Telescope (FACT, [1]) at the Observatorio del Roque de los Muchachos at the Canary Island of La Palma. It is the first focal plane installation based on silicon photo sensors. The camera, comprising 1440 individually read out channels, has been developed to prove the applicability of Geiger-mode avalanche photodiodes as focal plane photo sensors, but also to serve as a monitoring device at TeV energies for the brightest known blazars.

While the number of bright sources is limited, the number of different environmental conditions during data taking is infinite. To optimize the distribution of observation time between the possible sources, in terms of sampling density, understanding the relation between the observation conditions and the energy threshold, respectively sensitivity, is important.

2 Concept

Cherenkov telescopes record nano-second light flashes from the Cherenkov light emitted by particle cascades in the atmosphere. Primary gamma-rays induce electromagnetic showers for which the density of the emitted photons, in the first order, is directly proportional to the energy of the primary photon. The total number seen by the telescope camera is therefore a direct measure of the energy as well. Since electromagnetic showers are highly collimated along the direction of the primary particle, and therefore have a well defined geometry, also the signal density correlated

with the primary energy. Therefore, the trigger threshold of the telescope can also be interpreted as an energy threshold.

During observation the zenith angle of the observed source is changing. With increasing zenith angle, the distance between the shower core, i.e. the height at which most of the light is emitted, and ground is increasing. The light density on ground and with it the light yield measured by the telescope is decreasing. This increases the corresponding energy at the trigger threshold.

The trigger threshold is determined by triggers from random coincidences of photons from background light, mainly the diffuse night-sky background and moon light, but is also influenced by atmospheric conditions like dust in the air or clouds.

As the ideal trigger threshold, usually the point is assumed at which the rate from these random triggers becomes negligible compared to the rate induced by showers from the mainly hadronic background. Due to a very strong dependence of the trigger rate induced by artificial coincidences of the background photons from the trigger threshold, this point can be considered independent from the zenith angle and the highest background spectrum close to zenith can be assumed.

If the zenith angle, and therefore the conversion factor from light yield to energy is known and the increase of the trigger threshold can be predicted from the expected light conditions, the change in energy threshold can also be predicted.

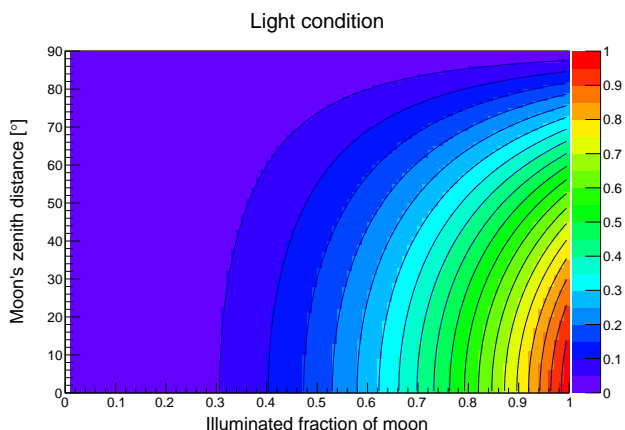


Figure 1: Light condition. As color scale, a value describing the background light condition is plotted versus the moon's illuminated fraction and the moon's zenith angle. It is proportional to the measured median current in the camera. Each contour level corresponds to a step of 0.05. The values range from new moon condition (0) to the worst possible condition at full moon (1).

3 Current prediction

To be able to predict the trigger threshold, in a first step, the flux of background photons must be known. Since this flux is dominated by moon light, and represented by the measured current in the camera, a correlation between those two is searched. Of course, the existence of such a correlation depends on the stability of the gain of the photo sensors. The stability is discussed in [2, 3].

Empirically, a correlation between the moon-brightness, expressed as the illuminated fraction of the moon's disc and its zenith angle, and the measured median current in the camera could be found. Further correlations, for example, of the current from the distance between the object and the moon or the object's zenith angle are very weak in the dataset used. For the study, a careful data selection has been done to avoid any bias from atmospheric conditions, e.g. dust, or weather conditions like clouds. Under real observation conditions, which are not always ideal, the current might still be higher than the predicted value, but should by no means be lower.

In Fig. 1 a value, called *light condition* directly derived from the moon properties and proportional to the median current is shown. While a value of zero corresponds to new moon condition, a value of one would correspond to full moon with the moon at zenith.

A more detailed discussion can be found in [3] and soon in [4].

4 Trigger threshold prediction

To convert the predicted current into a trigger threshold, the function describing the threshold dependency of the rate must be parametrized as a function of the current. To do this, the dependence of the rate from the threshold has been measured at different light conditions at ideal atmospheric conditions and close to zenith. The effect of atmospheric conditions on ratescans is discussed in [5].

In Fig. 2 (top) some exemplary ratescans are shown. After the counter got out of saturation, the fast decrease

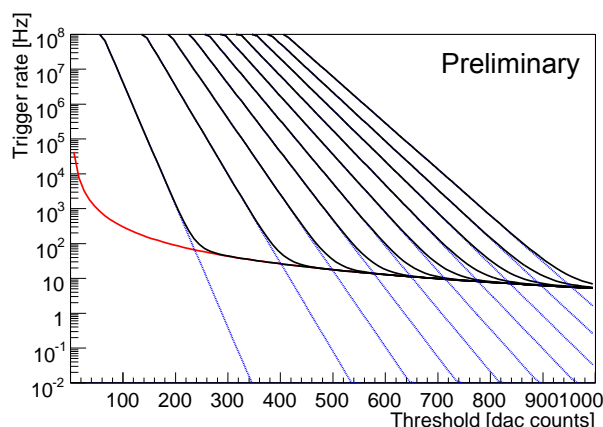
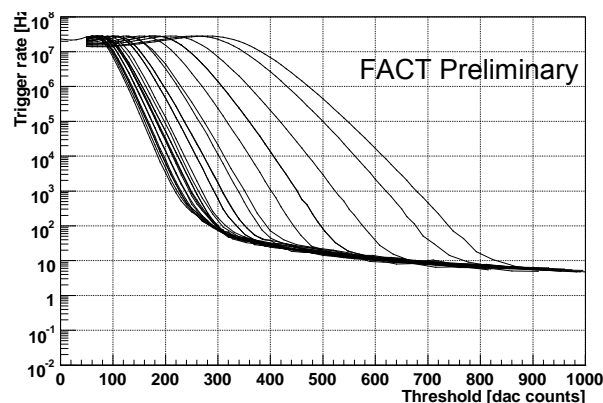


Figure 2: Top: Ratescans taken close to zenith at different light conditions between dark night conditions and almost full moon conditions. Bottom: Parametrization for ratescans depending on the measured median current with $10\mu\text{A}/\text{ch}$ spacing. The power-law of the proton spectrum (red) and the background spectra (black).

of random coincidences with raising trigger threshold is visible and the transition to the spectrum of coincident triggers from background showers. While the background spectrum is independent of the background light, the shift of the falling edge between new moon conditions (left) and almost full moon conditions (illuminated fraction 90%, right) is obvious. The falling edge has been parametrized by means of linear regression between 10^3Hz and 10^4Hz . The spectrum of background shower has been parametrized by a power-law. Knowing the background spectrum is totally dominated by hadron induced showers and knowing their spectral index, compatible with the fit result, the power-law index has been fixed to -1.7 to reduce the number of free parameters. Fig. 2 (bottom) shows the result of the parametrization for a spacing in current of $10\mu\text{A}/\text{ch}$.

From this parametrization, the ideal trigger threshold is derived as the point at which the random trigger rate has fallen $1/e$ -th below the trigger rate from hadron showers. The resulting current dependent trigger threshold is now in use during standard data taking since several months. Before each data run, which usually lasts five minutes, the median current is readout and the corresponding trigger threshold set. Except the influence of bright stars in the field-of-view, the threshold is then kept constant during these five minutes of data taking, to allow for easier analysis of the data.

Before this method of setting the threshold was imple-

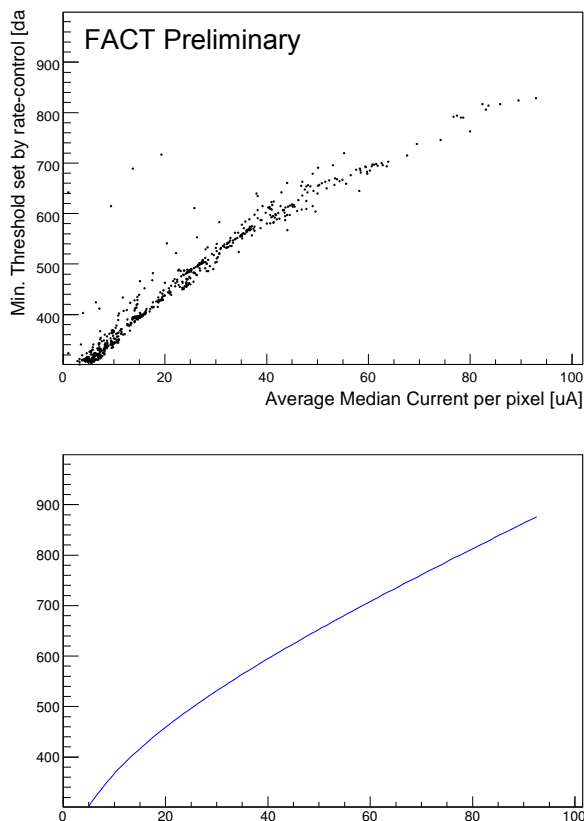


Figure 3: Top: Threshold to archive a trigger rate below 70 Hz as determined by a mini-ratescan versus median current, applied for several month before each 5 min data run. Bottom: Trigger threshold depending on median current determined from the parametrized ratescans shown at the top in Fig. 2 (bottom) for a fixed rate of 70 Hz. A good agreement with the measurement in the top figure is visible.

mented, the trigger threshold during data taking was determined by a kind of mini ratescan before each run, which effectively increased the trigger threshold until the rate had dropped below 70 Hz. The obtained correlation between threshold and median current is shown in Fig. 3 (top). For comparison, Fig. 3 (bottom) shows the same but obtained from the parametrization shown in Fig. 2 (bottom).

Taking the proportionality between the energy and the light yield into account, it can be assumed that the trigger threshold and the energy threshold are proportional as well. Therefore, the obtained parametrization can be used to derive the worsening of the energy threshold with increase in current. The previously obtained correlation, allows to directly correlate the energy threshold with the moon properties.

5 Energy threshold prediction

To adapt the obtained energy threshold to the zenith angle of the source, the decrease of light density on the ground with increasing zenith angle has to be taken into account.

This effect can either be calculated or simulated. A Monte Carlo simulation how the energy threshold changes with zenith angle at constant trigger threshold can be found in [6]. The data obtained from this study is shown in Fig. 4

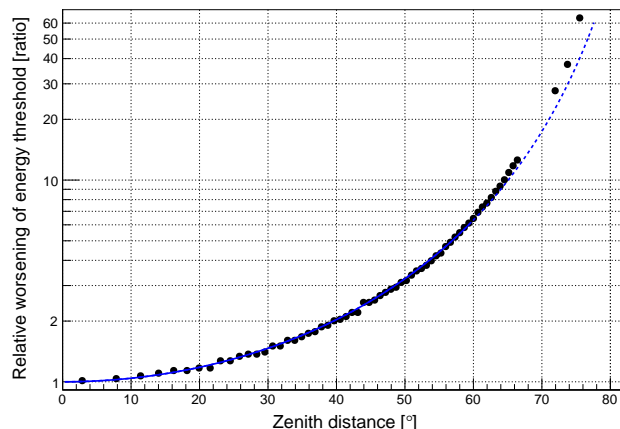


Figure 4: Relative worsening of the energy threshold expressed as a ratio versus the zenith angle θ . The black points are simulation results for the MAGIC telescope and were taken from [6]. A fit to the data (up to 60° zenith angle) in $\cos^\alpha \theta$ is overlaid as blue line.

as a relative change of energy threshold versus zenith angle. The data was fitted with $\cos^\alpha \theta$ yielding $\alpha = -2.66$ which is overlaid as blue line. Although, geometrically a square dependence is expected, this result is worsened by the increase of absorption due to the longer path length at higher zenith angles. For the fit, only data points up to 60° zenith distance were taken into account, because starting around this angle, it makes a significant difference for the result whether a curved or flat atmosphere is assumed in the simulation. According to the description of the simulation, the curved atmosphere was not switched on in the simulation, which results in an energy threshold at high zenith angles worse than expected. However, the difference up to 70° zenith distance is still at the few percent level and can be neglected. Observations above 70° would anyway only be scheduled in exceptional cases in which the precise decrease in energy threshold is not expected to be the primary criteria anymore.

Although, strictly speaking, this result is not valid for the FACT telescope because it was obtained for the MAGIC telescope, no major difference between both is expected under the assumption that the total light yield corresponding to a given trigger threshold does not significantly change with zenith angle.

6 Result

Both results, the increase of the trigger threshold as shown in 3 depending on the moon's properties, and the increase of energy threshold depending on the zenith angle of the source can now be combined into a single prediction for the worsening in energy threshold. This worsening is shown in Fig. 5. The relative increase in energy, i.e. worsening in energy threshold, is shown as a color scale versus the light condition and zenith angle of the observed source. A light condition of 0 corresponds to new moon conditions, while a light condition of 1 would correspond to full moon with the moon at zenith. The full dependency of the light condition on moon brightness and zenith angle is shown in Fig. 1. It can be seen that at very bright condition, the brightness dominates the energy threshold while at high zenith angles, the background light level has only a minor influence.

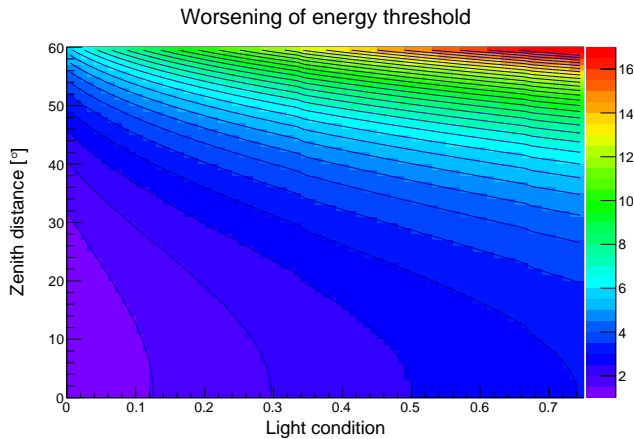


Figure 5: Worsening of energy threshold color coded expressed as a ratio of energies versus light condition and the zenith angle of the observed source. Light condition 0 corresponds to a new moon night, light condition 1 would correspond to a full moon night with the moon at zenith. The full dependency is shown in Fig. 1. Each contour level corresponds to a step of 0.5. For example, comparable energy thresholds are expected for a light condition of 0.75 close to zenith and at 50° zenith angle at dark night. A light condition of 0.75 corresponds to the moon illuminated by not more than 75% also close to zenith.

7 Conclusion

With the FACT telescope, the first complete focal plane installation using silicon photo sensors is available. It was proven that even under real observation conditions like changing weather and light conditions, a stable operation is possible within the limits of the calibration of the bias voltage.

Using this stability, it was possible to predict the current as a representation for the photon flux from the diffuse background light depending on light conditions, i.e. depending on the moon's zenith angle and brightness.

This prediction was then correlated with the measured rate depending on the trigger threshold setting allowing. This enables the use of the measured median current in the camera to define the global trigger threshold during observation which has turned out to be a very stable and robust procedure.

Given that the threshold is closely correlated to a local light density in the camera and that gamma showers, especially at the trigger threshold, are very well concentrated, the trigger threshold is equivalent to a measured energy.

Putting this result together with the change in energy threshold coming from the change in light density with different observation zenith angles, yield a prediction of the worsening of the energy threshold with light condition and zenith angle.

Since the main physics goal of the FACT telescope is the long-term monitoring of bright TeV blazars (mainly Mrk 421 and Mrk 501) the prediction of the energy threshold is important to allow for the optimum balance in sampling density with their quiescent flux as reference.

Given the stability of the system and the possibility to optimize the physics output, the FACT telescope does not only prove the applicability of silicon photo sensor in focal planes and especially in Cherenkov telescopes, it is also

an ideal instrument to gain knowledge on the long-term behavior of the brightest blazars.

An overview of the telescope hardware and software is given in [1]. An detailed discussion of the stability will be available soon in [4].

Acknowledgment The important contributions from ETH Zurich grants ETH-10.08-2 and ETH-27.12-1 as well as the funding by the German BMBF (Verbundforschung Astro- und Astroteilchenphysik) are gratefully acknowledged. We are thankful for the very valuable contributions from E. Lorenz, D. Renker and G. Viertel during the early phase of the project We thank the Instituto de Astrofisica de Canarias allowing us to operate the telescope at the Observatorio Roque de los Muchachos in La Palma, and the Max-Planck-Institut für Physik for providing us with the mount of the former HEGRA CT3 telescope, and the MAGIC collaboration for their support. We also thank the group of Marinella Tose from the College of Engineering and Technology at Western Mindanao State University, Philippines, for providing us with the scheduling web-interface.

References

- [1] H. Anderhub et al. (FACT Collaboration), 2013, JINST **8** P06008 [arXiv:1304.1710].
- [2] T. Bretz et al. (FACT Collaboration), these proc., ID 683.
- [3] M. Koetig et al. (FACT Collaboration), these proc., ID 695.
- [4] FACT Collaboration, *in prep.*
- [5] D. Hildebrand et al. (FACT Collaboration), these proc., ID 709.
- [6] R. Firpo, thesis, IFAE/UAB 2006.
- [7] T. Bretz et al. (FACT Collaboration), these proc., ID 682.